JOURNAL OF AGRICULTURAL AND FOOD CHEMISTRY

Tomato Metabolism and Porphyrin-Catalyzed Oxidation of Pyriproxyfen

MASAO FUKUSHIMA,* TAKUO FUJISAWA, AND TOSHIYUKI KATAGI

Environmental Health Science Laboratory, Sumitomo Chemical Co., Ltd., 2-1 Takatsukasa 4-chome, Takarazuka, Hyogo 665-8555, Japan

Investigation of the metabolism of [^{14}C]pyriproxyfen [4-phenoxyphenyl (*R*,*S*)-2-(2-pyridyloxy)propyl ether] in tomato fruits (*Lycopersicon esculentum* Mill. cv. Ponterosa) was conducted by topical application of acetonitrile solution or emulsifiable concentration formulation three times at 35, 21, and 7 days before harvest. Most of the radioactivity remained on the fruit surface or in the plant tissues as intact pyriproxyfen with minor metabolites formed via hydroxylation at the 4′-position of the phenoxy ring or cleavage of ether linkages. The biomimic chemical oxidation model using iron porphyrin as a catalyst and hydrogen peroxide was found to well reproduce the primary metabolites detected in the metabolism study. The electrophilic reaction indices obtained by AM1 molecular orbital calculations supposing involvement of cytochrome P-450 were successfully applied to evaluate the potentially higher reactive sites in pyriproxyfen.

KEYWORDS: Pyriproxyfen; metabolism in *Lycopersicon esculentum*; porphyrin-catalyzed oxidation

INTRODUCTION

Pyriproxyfen (**1**) [4-phenoxyphenyl (*R*,*S*)-2-(2-pyridyloxy)-propyl ether] is an insect growth regulator (IGR) having a high biological activity against flies, mosquitoes, and cockroaches (*1*, *2*). IGRs are expected to be used for integrated pest management to avoid insecticide resistance, and some of them are presently being used to manage the insects in many countries (*3*). The metabolism of **1** in aquatic organisms together with its ecological effect has been reviewed by Miyamoto et al. (*3*), and that in rats and mice was reported by Matsunaga et al. (*4*) and Yoshino et al. (*5*, *6*) in more detail. Moreover, in vitro metabolism of **1** by microsomes prepared from housefly larvae was also investigated (*7*), but the metabolism in plants has not been examined yet. Microsomal cytochrome P-450 (CYP) is recognized as one of the most important key enzymes in the metabolism of xenobiotics, and various approaches have been developed to determine their potential metabolites or to collect them for an effective development of drugs (*8*). Among them, catalytic oxidation by synthetic metalloporphyrins has been frequently applied to many drugs (*8*) for the reason of simple and reproducible experimental procedures. The polyhalogenated metalloporphyrins substituted at the *meso*- and β-positions are known as efficient models for biomimic oxidation catalyzed by CYP (*9*). It has been also demonstrated by Keserü (*10*) that oxidation profiles of carbofuran with *meso*-tetrakis(pentafluorophenyl)porphyrin iron(III) chloride in the presence of hydrogen peroxide are in good agreement with those of its in vivo metabolism in housefly (*Musca domestica*). Therefore, we conducted plant metabolism of [^{14}C]-**1** in tomato fruit together with the catalytic oxidation by metalloporphyrins to determine its metabolic profiles and the applicability of a chemical oxidation model system. Furthermore, molecular orbital calculations were conducted to determine the essential reactivity of **1** in conjunction with metabolism and catalytic oxidation.

MATERIALS AND METHODS

Chemicals. Non-radiolabeled authentic standards of **1** and the following potential metabolites were synthesized in our laboratory according to the reported methods (*3*−*5*): (*R*,*S*)-5-hydroxy-2-{1-methyl-2-(4-phenoxyphenoxy)}ethoxypyridine (**2**), 4-(4-hydroxyphenoxy)-phenyl (*R*,*S*)-2-(2-pyridyloxy)propyl ether (**3**), (*R*,*S*)-2-hydroxypropyl 4-phenoxyphenyl ether (**4**), 4-phenoxyphenol (**5**), 4-hydroxyphenyl (*R*,*S*)-2-(2-pyridyloxy)propyl ether (**6**), 4-(4-hydroxyphenoxy)phenyl (*R*,*S*)-2-hydroxy propyl ether (**7**), 4,4′-oxydiphenol (**8**), 4-hydroxyphenyl (*R*,*S*)-2-hydroxypropyl ether (**9**), (*R*,*S*)-2-(2-pyridyloxy)propionic acid (**10**), and (*R*,*S*)-2-(2-pyridyloxy)propyl alcohol (**11**). The two radiolabels of **1** were prepared in our laboratory (*11*) and used for both metabolism and chemical oxidation studies. [*phenoxyphenyl*-^{14}C]-**1** was uniformly labeled with ^{14}C at the phenoxyphenyl ring with a specific activity of 12.4 MBq mg^{-1}. [*pyridyl*-2,6-^{14}C]-**1** was labeled at the 2- and 6-positions of the pyridyl ring with a specific activity of 14.8 MBq mg^{-1} (**Figure 1**). The radiochemical purity of each radiolabel and the chemical purity of each potential metabolites were >99.2% and >99.1%, respectively, as determined by high-performance liquid chromatography (HPLC) linked with a radiodetector. 5,10,15,20-Tetrakis(pentafluorophenyl)-21*H*,23*H*-porphine iron(III) chloride (FeTPPF$_{20}$) was used in biomimic catalytic oxidation of **1**. FeTPPF$_{20}$ was purchased from Sigma-Aldrich Japan Co. Ltd. (Tokyo, Japan) and used without further purification. Other reagents were of the purest grade (99%) from Nacalai Tesque, Inc. (Kyoto, Japan).

Chromatograpy. HPLC analysis was conducted using a Hitachi L-6200 pump linked in series with an L-4000 UV detector, a D-7000 Advanced HPLC system manager, and a Packard Flow-one/Beta A-120 radiodetector equipped with a 500 mL liquid cell, where Ultima-Flo AP (Perkin-Elmer Japan Co.) was utilized as a scintillator. Sumipax

10.1021/jf0503816 CCC: $30.25
Published on Web 05/28/2005

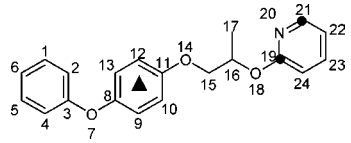

Figure 1. Chemical structure of pyriproxyfen (**1**) and its labeled positions: ▲, [*phenoxyphenyl*-^{14}C]-**1**; ●, [*pyridyl*-2,6-^{14}C]-**1**.

Table 1. Chromatographic Properties of Pyriproxyfen (**1**) and Its Potential Metabolites

compd	HPLC retention times (min)	TLC R_f values	
		system A[a]	system B[b]
1	37.1	0.84	0.72
2	33.6	0.58	0.62
3	32.7	0.59	0.63
4	29.6	0.60	0.53
5	28.4	0.56	0.65
6	26.5	0.54	0.61
7	24.1	0.41	0.49
8	22.7	0.37	0.56
9	18.6	0.35	0.45
10	20.0	0.09	0.45
11	16.6	0.53	0.40
12	3.4	0.23	0.20

[a] Chloroform/methanol = 9:1 (v/v). [b] Toluene/ethyl acetate/acetic acid = 5:7:1 (v/v/v).

ODS A-212 (150 mm × 6 mm i.d., 5 μm, SCAS Co., Ltd.) and YMC ODS AM-324 (300 mm × 10 mm i.d., 5 μm, YMC Co., Ltd.) columns were employed for analytical and preparative purposes at a flow rate of 1 and 2 mL min^{-1}, respectively. The following linear gradient solvent program was used for typical analysis of metabolites using the Sumipax ODS A-212 column with 0.01% trifluoroacetic acid (solvent A) and acetonitrile (solvent B): 0 min, 95% A−5% B; 5 min, 95% A−5% B; 35 min, 0% A−100% B; 45 min, 0% A−100% B. Thin-layer chromatography (TLC) was conducted using silica gel 60F_{254} thin-layer chromatoplates (20 cm × 20 cm, 0.25 mm thickness, E. Merck). The following solvent systems were used for two-dimensional development: chloroform/methanol, 9:1 (v/v); toluene/ethyl acetate/acetic acid, 5:7:1 (v/v/v). The non-radiolabeled reference standards were detected by exposing TLC plates to ultraviolet light. Autoradiograms were prepared by exposing TLC plates to a BAS-IIIs Fuji imaging plate for several days. The radioactivity on an imaging plate was detected by an Amersham Biosciences Typhoon 9200 scanner. The retention time (t_R) and R_f values of each chemical are summarized in **Table 1**.

Metabolism Study. Tomato seedlings (*Lycopersicon esculentum* Mill. cv. Ponterosa) in the fourth-leaf stage grown in compost (Kureha Chemical Co., Ltd., Tokyo, Japan) were transplanted to the 0.02-m^2 Wagner pot filled with either Takarazuka soil (sandy loam) or compost mixed with magnesia lime. Tomato plants were grown in a greenhouse (November 2003−February 2004) kept at 25/20 °C for day/night and appropriately watered until harvest for ∼3 months.

[^{14}C]-**1** was topically applied to fruit three times in the following solutions at a rate of 60 g of active ingredient acre^{-1} with an interval of 2 weeks between applications. The first application was conducted at the fruit growth stage of BBCH 85 (35 days before harvest), and the preharvest interval (PHI) was set as 7 days. The acetonitrile solution was used for investigation of the potential metabolism, and the emulsifiable concentrate was used to assess the metabolic profiles under the practical agricultural situation. [^{14}C]-**1** (111.9 μg) was diluted with non-radiolabeled **1** (2.126 mg; purity, 99.2%) in 2.13 mL of acetonitrile (specific activities of [*phenoxyphenyl*-^{14}C]-**1**, 0.62 MBq mg^{-1}; [*pyridyl*-2,6-^{14}C]-**1**, 0.74 MBq mg^{-1}). In the case of emulsifiable concentrate (EC), 55.95 μg of [^{14}C]-**1**, 1.06 mg of non-radiolabeled **1** (purity, 99.2%), and emulsifier Sorpol 3544X (Toho Chemical Industry Co., Ltd.) were dissolved in 11.19 μL of xylen. The emulsifiable concentrate of [^{14}C]-**1** was then diluted by 100-fold with deionized water. The surface area of fruit was calculated to be 50.3 cm^2 from its radius of 2 cm by assuming a spherical shape. About 70 μL ([*phenoxyphenyl*-^{14}C], 0.14 MBq; [*pyridyl*-^{14}C], 0.16−0.17 MBq) of each dosing solution was topically applied with a microsyringe to four tomato fruits. The radiochemical and chemical purities of all application solutions were measured immediately before and after each application, and no decrease of purities was found during this study.

Tomato fruits were sampled, weighed, and stored in a freezer (<−20 °C) until analysis. After the surface rinse with 50 mL of acetonitrile using a pipet for ∼1 min, each tomato fruit was crushed in the stainless steel cup of a Nissei Excel Auto homogenizer at 10000 rpm and 0 °C for 10 min without any solvent. The juice was collected by filtration of the homogenate. The pomace was extracted three times with 300 mL of acetone/water (4:1, v/v) under homogenization in the same condition as above, and the vacuum filtrates were combined for further analysis. The aliquots of surface rinse, juice, and extract of pomace were individually mixed with 10 mL of Emulsifier Scintillator Plus (Perkin-Elmer) and radioassayed by liquid scintillation counting (LSC) with a model 2900TR spectrometer (Perkin-Elmer), the detection limits of which for [*pyridyl*-2,6-^{14}C]-**1** and [*phenoxyphenyl*-^{14}C]-**1** were 0.004 and 0.002 ppm, respectively. The chemical- and color-quenching were not observed when the volume of the aliquot was ≤0.5 mL for juice or pomace with or without radiolabeled material. Therefore, the volume of aliquot of juice and pomace was ≤0.5 mL to avoid the color- or chemical-quenching. These aliquots were then subjected to HPLC and two-dimensional TLC cochromatographic analyses with authentic standards. Pulp residues were air-dried in an open vessel at room temperature overnight. The subsamples of dried residues were subjected to combustion analysis to determine the remaining radioactivity by using a Packard model 307 sample oxidizer. The $^{14}CO_2$ produced was absorbed into 9 mL of Carb-CO_2 absorber (Perkin-Elmer) and mixed with 15 mL of Permafluor scintillator (Perkin-Elmer), and the radioactivity in it was quantified by LSC. The values of background and the efficiency of combustion were 49 dpm and >91%, respectively. The unknown metabolites in juice and extract of pomace were individually isolated by HPLC. A subsample of each isolated fraction with a total radioactivity of ∼200 000 dpm was then hydrolyzed with 1 mL of 12 M hydrochloride at 80 °C for 2 h, followed by HPLC cochromatographic analysis with authentic standards to examine released aglycon.

Biomimic Oxidation Model. [^{14}C]-**1** (0.5 μmol) and $FeTPPF_{20}$ (0.024 μmol) were dissolved in 500 μL of chloroform/methanol (1:1, v/v) and 70−140 μmol of H_2O_2 was added. The reaction mixture was stirred for 10 min at room temperature, and the reactant was directly analyzed by HPLC cochromatography with authentic standards.

Molecular Orbital (MO) Calculations. The initial molecular geometry of **1** was derived from the standard values of bond lengths and angles. There are seven internal rotations along the molecular skeleton of **1**, and many conformers can exist in a lower energy state. Because the AM1 calculations of the pyrethroid model ester processing the diphenyl ether moiety showed an insignificant effect by conformation on the energy level of the highest occupied molecular orbital (HOMO) and its electron distribution (*12*), the extended conformation was conveniently taken for **1** by referring to the optimized conformation of the pyrethroid model ester. The *S*-configuration was conveniently chosen here from two optical isomers at C_{16}. The molecular geometries were then fully optimized by the AM1 method (*13*) using EF and PRECISE keywords in the WINMOPAC program (version 3.9, Fujitsu Ltd.).

It is considered that the metabolic oxidation of pesticides in the tissues is catalyzed by oxidases such as cytochrome P-450 (CYP) (*14*), and the reaction site of CYP, oxo-iron(IV) porphyrin cation radical, possesses an electron-deficient character (*15*). The electrophilic reaction index (f_E) for each atom of **1** calculated by the electron distribution of HOMO and the neighboring occupied MOs with the following equation is suitable for evaluation of the oxidizable sites by oxidases (*16*).

$$f_E = 2\sum(C_i^j)^2 \qquad (i = s, p_x, p_y, p_z)$$

Here, C_i^j is the coefficient of the ith atomic orbital in the jth MO including HOMO for each atom. An atom having a larger f_E value is considered to be more susceptible to metabolic oxidation.

Table 2. Distribution of Radioactivities and Metabolites in Tomato Fruit[a]

	acetonitrile solution				emulsifiable concentrate solution			
	[PH][b]		[PY][b]		[PH]		[PY]	
compound	% TRR	ppm[c]	% TRR	ppm[c]	% TRR	ppm[c]	% TRR	ppm[c]
surface	**73.65**	**3.269**	**60.15**	**2.918**	**12.40**	**0.601**	**13.46**	**0.435**
1	72.46	3.216	59.82	2.902	11.86	0.575	13.16	0.425
2	nd	nd	nd	nd	nd	nd	nd	nd
3	nd	nd	nd	nd	0.06	0.003	0.02	0.001
4	nd	nd	–	–	nd	nd	–	–
5	nd	nd	–	–	nd	nd	–	–
6	nd	nd	nd	nd	nd	nd	nd	nd
7	nd	nd	–	–	nd	nd	–	–
8	nd	nd	–	–	nd	nd	–	–
9	nd	nd	–	–	nd	nd	–	–
10	–	–	nd	nd	–	–	nd	nd
11	–	–	nd	nd	–	–	nd	nd
12	–	–	nd	nd	–	–	nd	nd
others	1.19	0.053	0.33	0.016	0.47	0.023	0.29	0.009
juice	**1.59**	**0.074**	**2.68**	**0.182**	**0.84**	**0.048**	**1.06**	**0.049**
1	0.79	0.039	1.37	0.093	0.43	0.024	0.58	0.027
2	nd	nd	nd	nd	nd	nd	nd	nd
3	nd	nd	nd	nd	nd	nd	nd	nd
4	nd	nd	–	–	nd	nd	–	–
5	0.02	0.001	–	–	nd	nd	–	–
6	nd	nd	nd	nd	nd	nd	nd	nd
7 (conj)[d]	0.06	0.003	–	–	nd	nd	–	–
8	nd	nd	–	–	nd	nd	–	–
9 (conj)[d]	0.05	0.002	–	–	0.03	0.002	–	–
10	–	–	nd	nd	–	–	nd	nd
11	–	–	nd	nd	–	–	nd	nd
12	–	–	nd	nd	–	–	nd	nd
others	0.66	0.032	1.31	0.089	0.41	0.023	0.49	0.022
pomace extract	**24.19**	**1.132**	**35.71**	**2.701**	**79.32**	**4.866**	**74.46**	**3.232**
1	22.24	1.041	31.52	2.384	75.66	4.642	71.97	3.124
2	nd	nd	nd	nd	nd	nd	nd	nd
3	0.28	0.013	1.06	0.080	1.03	0.063	1.13	0.049
4	0.13	0.006	–	–	0.10	0.006	–	–
5	nd	nd	–	–	0.03	0.002	–	–
6	nd	nd	0.14	0.011	nd	nd	nd	nd
7	0.01	0.001	–	–	nd	nd	–	–
8	nd	nd	–	–	nd	nd	–	–
9	nd	nd	–	–	nd	nd	–	–
10	–	–	0.18	0.014	–	–	nd	nd
11	–	–	0.08	0.006	–	–	nd	nd
12	–	–	nd	nd	–	–	nd	nd
others	1.53	0.07	2.74	0.207	2.50	0.153	1.36	0.059
pomace unextractable	**0.58**	**0.027**	**1.45**	**0.096**	**7.45**	**0.623**	**11.01**	**0.566**
total	**100.00**	**4.502**	**100.00**	**5.897**	**100.00**	**6.138**	**100.00**	**4.282**
recovery of applied ^{14}C	**81.36**		**81.23**		**84.78**		**86.54**	

[a] All values are averages of quadruplicate. [b] [PH], [*phenoxyphenyl*-^{14}C]-**1**; [PY], [*pyridyl*-2,6-^{14}C]-**1**. [c] Equivalent of **1**. [d] These aglycons were released by acidic hydrolysis. nd: Not detected. –: No formation from radiolabel used.

RESULTS

Tomato Metabolism Study. When the acetonitrile solution of [^{14}C]-**1** was applied to tomato fruit, the recovered radioactivity from rinse, juice, and pomace in total ranged from 73.0 to 93.5%, and the average of four replicates was ~81% of the nominally applied ^{14}C. Approximately 60−74% of total radioactive residues was present in the surface rinse fraction. All of the radioactivity recovered from the surface rinse was unaltered **1**. As summarized in **Table 2**, the extent of metabolism of **1** in tomato fruits was small (4.5−7.3% TRR), and some metabolites were detected in the fraction of juice and extract of pomace. In the case of the treatment with [*phenoxyphenyl*-^{14}C]-**1**, **5** was found as a free metabolite and **7** and **9** were found as conjugates in the juice fraction. **3**, **4**, and **7** were found as free metabolites from the extract of pomace. These conjugates were considered to be conjugated with natural components such as sugars or amino acids because of the release of their aglycons by acidic hydrolysis. **6** was a common metabolite of two [^{14}C]-**1** labels but was not detected from the pomace of [*phenoxyphenyl*-^{14}C]-**1**. When [*pyridyl*-^{14}C]-**1** was applied, **10** and **11** characteristic to this label were detected in addition to the common metabolites **3** and **6** in the extract of pomace. The acidic hydrolysis of unknown metabolites in the juice fraction was not effective for the release of aglycon. On the other hand, the use of the EC of [^{14}C]-**1** greatly reduced the radioactive residues to 4.0−21.3% on the fruit surface, with a ^{14}C recovery of ~85%. In this case, the extracts from pomace showed predominant radioactivity as listed in **Table 2**. Although the extent of metabolic degradation was small, more formation of the common metabolite **3** (1.0−1.1%) was observed in the extract of pomace from both radiolabels together with **4** and **5** as free metabolites from [*phenoxyphenyl*-^{14}C]-**1**. The trace amount of **9** was released by acidic hydrolysis of the juice fraction from [*phenoxyphenyl*-^{14}C]-**1**. Different from the application of the acetonitrile solution, no trace amount of the known metabolites could be detected from the treatment with [*pyridyl*-^{14}C]-**1**. Irrespective of the

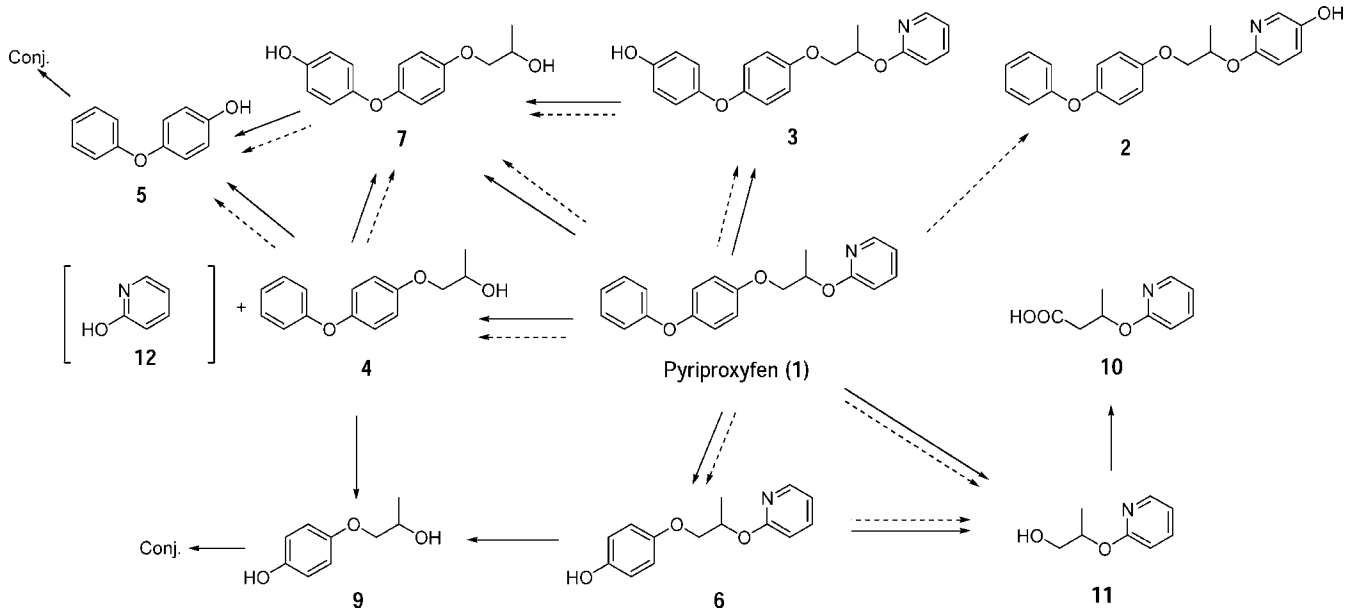

Figure 2. Proposed metabolic pathways of pyriproxyfen (**1**) in tomato fruit and porphyrin-catalyzed oxidation: solid arrow, plant metabolism; broken arrow, porphyrin-catalyzed oxidation.

Table 3. Oxidative Metabolites Catalyzed by Biomimic Oxidation Model

	% of recovered ^{14}C			% of recovered ^{14}C	
compd	[PH][a]	[PY][a]	compd	[PH][a]	[PY][a]
1	nd	nd	**7**	7.8	–
2	4.2	–	**8**	nd	–
3	9.5	10.6	**9**	nd	–
4	14.2	–	**10**	–	nd
5	nd	–	**11**	–	33.1
6	31.5	10.9	**12**	–	nd

[a] [PH], [*phenoxyphenyl*-^{14}C]-**1**; [PY], [*pyridyl*-2,6-^{14}C]-**1**.

treatment solution, neither **2** nor **12** was detected in any fraction from tomato fruit. On the basis of the detailed metabolites, the metabolic pathways of **1** in tomato fruit are proposed in **Figure 2**. **1** primarily underwent hydroxylation at the 4′-position of the terminal phenoxyphenyl ring to form **3**, cleavage of the propylpyridyl ether to form **4**, cleavage at the propyl phenyl ether to form **11** and **5**, desphenylation, following conjugation of these metabolites.

Porphyrin-Catalyzed Oxidation. When [*phenoxyphenyl*-^{14}C]-**1** was oxidized by $FeTPPF_{20}$ and hydrogen peroxide, no trace amount of **1** remained after 10 min and **3** (9.5−10.6%) and **6** (10.9−31.5%) were predominantly detected as common metabolites to both radiolabels, as listed in **Table 3**. The label-specific metabolites **4** and **7** amounted to 14.2 and 7.8%, respectively. In addition to these metabolites, **2** via hydroxylation of **1** at the 5″-position of the pyridyl ring was also detected (4.2%). In the case of [*pyridyl*-^{14}C]-**1**, **11** (33.1%), **6** (10.9%), and **3** (10.6%) were produced. On the basis of product distribution, porphyrin-catalyzed oxidation of **1** was found to reproduce the primary reactions observed in tomato metabolism. **12** and **5** could not be detected, although the respective structural counterparts **4** and **11** were detected. Because these two potential metabolites possess the reactive hydroxy group, further rapid oxidation would be most likely to proceed.

MO Calculation. The optimized geometry of **1** gave the total energy of −3703.3786 eV and heat of formation of −22.157 kcal mol^{-1}. The torsional angles obtained were −177.9° ($\angle C_2C_3O_7C_8$, **Figure 1**), 88.7° ($\angle C_3O_7C_8C_9$), 0.2° ($\angle C_{10}C_{11}O_{14}C_{15}$), −165.9° ($\angle C_{11}O_{14}C_{15}C_{16}$), 169.8°($\angle C_{14}C_{15}C_{16}O_{18}$), 151.2° ($\angle C_{15}C_{16}O_{18}C_{19}$), and −11.3° ($\angle C_{16}O_{18}C_{19}N_{20}$). The ball-and-stick model of the molecular structure reflecting the determined torsion angles is shown in **Figure 3**. The energy levels of HOMO, HOMO+1, and HOMO+2 were calculated to be −9.091, −9.172, and −9.575 eV, respectively. For each MO, the f_E indices were calculated at each atom of **1**, as summarized in **Table 4**. About 52 and 31% of electrons in HOMO were localized at the phenoxy (C_1−C_6) and phenoxyphenyl (C_8−C_{13}) rings, respectively, and in the case of HOMO+1 the corresponding distributions were 34 and 50%.

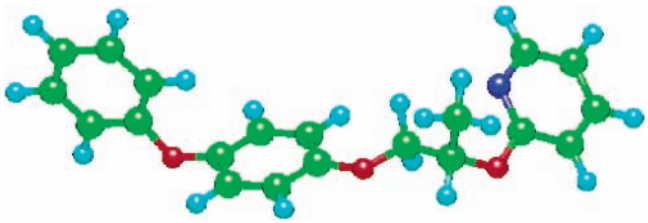

Figure 3. Ball-and-stick model of pyriproxyfen (**1**) reflecting the torsion angles at minimized energy: green, carbon atom; red, oxygen atom; blue, nitrogen atom; light blue, hydrogen atom.

Table 4. f_E Values of Pyriproxyfen (**1**) Calculated in Gas Phase

	$f_E = 2\Sigma(Ci)^2$			
	molecular orbital			molecular orbital
atom no.	HOMO	HOMO+1	atom no.	HOMO+2
C_1	0.069	0.047	C_{15}	0.015
C_2	0.138	0.084	C_{16}	0.006
C_3	0.289	0.203	C_{17}	0.017
C_4	0.163	0.100	O_{18}	0.316
C_5	0.042	0.029	C_{19}	0.352
C_6	0.334	0.213	N_{20}	0.110
O_7	0.215	0.119	C_{21}	0.223
C_8	0.202	0.325	C_{22}	0.543
C_9	0.041	0.038	C_{23}	0.008
C_{10}	0.078	0.166	C_{24}	0.405
C_{11}	0.158	0.252		
C_{12}	0.085	0.112		
C_{13}	0.054	0.089		
O_{14}	0.116	0.197		
C_{15}–C_{24}	<0.002	<0.004	C_1–C_{14}	<0.001

In contrast, most electrons in HOMO+2 were localized at the pyridyl ring (82%). Although the energy level of a reactive species in oxidases is not available, these three MOs were used for estimating the reaction sites in **1** due to their close energy levels. From the f_E indices, the reactive sites of **1** were estimated to be C_6 (4′-OH) > C_3 (1′-OH) > C_8 (4-OH) > C_{11} (1-OH) ≈ C_2, C_4 (2′-OH) for HOMO, $C_8 > C_{11} > C_3 \approx C_6$ for HOMO+1, and C_{22} (5″-OH) > C_{24} (3″-OH) > C_{19} (2″-OH) > C_{21} (6″-OH) for HOMO+2 (**Figure 1**; **Table 4**). The reactions at C_3 or C_8, C_6, and C_{19} are considered to lead to the formation of **6**, **3**, and **4**, respectively. Those at C_{11} and C_{22} give **11**, **5**, and **2**. Although the f_E indices proposed the reaction at the C_{21} and C_{24} positions of **1**, the corresponding metabolites could not be detected either in tomato metabolism or in porphyrin-catalyzed oxidation.

DISCUSSION

In the tomato fruit metabolism study using the EC formulation, more **1** penetrated into plant tissues as compared with the application of acetonitrile solution, although there were some variations between fruits. The surfactant in the formulation is known to facilitate penetration of pesticide from plant surface to tissues (*17*), which would result in the present differences in radiocarbon distribution between two applications, although the metabolic patterns in these applications are almost the same. Although the relative metabolic activity among each part of the tomato plant is not well-known, the new insecticide pyridalyl, having similar ether linkage in the molecule, showed less metabolic degradation in tomato fruit (*18*). In the case of a pesticide having an ester linkage, the ester cleavage by esterases predominantly proceeds when penetrated into tomato plants (*19*). However, such reactions are not operative for **1** due to the lack of an ester linkage, which seems to result in **1** as a major component of radiocarbons in juice and pomace extract fraction. The observed pathways in the metabolic and porphyrin-catalyzed oxidation reactions are similar to those in the mammalian metabolism studies in rats (*4*) and mice (*5*). In the feces, urine, and liver of rats and mice, **3** and its sulfate or glucuronide conjugate are the major metabolites. Besides them, the hydrooxylated derivatives of **1** at the 2′-position of the phenoxyphenyl ring, the 5″-position of the pyridyl ring (**2**), and both the 4′- and 5″-positions were also detected in rats and mice. When carp (*Cyrinus carpio*) was exposed to [^{14}C]-**1** at a concentration of 2 ppb, the major metabolic site was at the 4′-position of the phenoxyphenyl ring and the resultant phenol was conjugated with glucuronic acid or sulfuric acid (*3*). From an in vitro study in housefly (*Musca domestica* L.), most of the [^{14}C]-**1** remained as an intact form with formation of **2**, **3**, and **4**. Therefore, metabolic pathways of **1** seemed to be partly common among plants, mammals, fishes, and insects. As for the hydroxylation at the phenyl ring, a similar reaction has been reported for fenoxycarb (*20*) and some pyrethroids (*19*, *21*−*26*). These common profiles are supposed to be related to oxidases in plants.

The hydroxylation at the para-position of the phenyl ring by tomato was in accordance with the results in the detailed experiment examining the effect of a substituent on aromatic ring oxidation using *m*-chloroperbenzoic acid being catalyzed by $FeTPPF_{20}$ by Safari (*27*). Judging from the amount of each degradate, the present catalytic oxidation model had more hydroxylation ability at the 4′-position of the phenoxyphenyl ring than at the 2′- or 5″-position of the pyridyl ring. Because the three ether bonds of **1** were equally oxidized to form **4**, **6**, **7**, **9**, and **11**, there was no significant regioselectivity. As summarized in **Table 3**, the porphyrin-catalyzed oxidation seems to well reproduce the primary metabolites being detected in the tomato metabolism study, but the relative yields of these metabolites could not be estimated by the chemical oxidation. This quantitative difference is likely to be caused by mainly the interaction of substrate and enzymes or substrate specificity. However, this chemical oxidation model covers most kinds of in vivo metabolites, and it seems to be a highly credible and effective tool to predict the kinds of metabolites or degradates.

Incidentally, the theoretical approach using the f_E index was known as a convenient tool to estimate the possible sites of metabolic hydroxylation for synthetic pyrethroids (*28*) and also examined for biphenyls and diaromatics in comparison with metabolic profiles in mammals (*29*). Meanwhile, the steric constraints between the substrate and enzyme might give regioselective formation of metabolites, as reported for carbofuran (*30*). In this study, the sites having higher f_E values are mostly consistent with those where the metabolic and chemical transformation occurred. Therefore, this MO approach can be useful only in predicting the essential reactivity of pesticide, but there was no concrete relationship between f_E values and the degree of metabolic hydroxylation.

LITERATURE CITED

(1) Hatakoshi, M.; Kawada, H.; Nishida, S.; Kishida, H.; Nakayama, I. Laboratory evaluation of 2-[1-methyl-2-(4-phenoxyphenoxy)-ethoxy]pyridine against larvae of mosquitoes and housefly. *Jpn. J. Sanit. Zool.* **1987**, *38*, 271−274.

(2) Kawada, H.; Dohara, K.; Shinjo, G. Evaluation of larvicidal potency of insect growth regulator, 2-[1-methyl-2-(4-phenoxyphenoxy)ethoxy]pyridine, against the housefly, *Musca domestica*. *Jpn. J. Sanit. Zool.* **1987**, *38*, 317−322.

(3) Miyamoto, J.; Hirano, M.; Takimoto, Y.; Hatakoshi, M. Insect growth regulators for pest control, with emphasis on juvenile hormone analogs. In *Pest Control with Enhanced Environmental Safety*; Duke, S. O., Menn, J. J., Plimmer, J. R., Eds.; ACS Symposium Series 524; American Chemical Society: Washington, DC, 1993; Chapter 11, pp 144−168.

(4) Matsunaga, H.; Yoshino, H.; Isobe, N.; Kaneko, H.; Nakatsuka, I.; Yamada, H. Metabolism of pyriproxyfen in rats. 1. Adsorption, disposition, excretion, and biotransformation studies with [*phenoxyphenyl*-^{14}C]pyriproxyfen. *J. Agric. Food Chem.* **1995**, *43*, 235−240.

(5) Yoshino, H.; Kaneko, H.; Nakatsuka, I.; Yamada, H. Metabolism of pyriproxyfen. 2. Comparison of in vivo metabolism between rats and mice. *J. Agric. Food Chem.* **1995**, *43*, 2681−2686.

(6) Yoshino, H.; Kaneko, H.; Nakatsuka, I.; Yamada, H. Metabolism of pyriproxyfen. 3. In vitro metabolism in rats and mice. *J. Agric. Food Chem.* **1996**, *44*, 1578−1581.

(7) Zhang, L.; Kasai, S.; Shono, T. *In vitro* metabolism of pyriproxyfen by microsomes from susceptible and resistant housefly larvae. *Arch. Insect Biochem. Physiol.* **1998**, *37*, 215−224.

(8) Bernadou, J.; Meunier, B. Biomimetic chemical catalysts in the oxidative activation of drugs. *Adv. Synth. Catal.* **2004**, *346*, 171−184.

(9) Dolphin, D.; Traylor, T.; Xie, L. Y. Polyhaloporphyrins: unusual ligands for metals and metal-catalysed oxidations. *Acc. Chem. Res.* **1997**, *30*, 251.

(10) Keserü, G. M.; Balogh, G.; Czudor, I.; Karancsi, T.; Fehér, A.; Bertók, B. Chemical models of cytochrome P450 catalyzed insecticide metabolism. Application to the oxidative metabolism of carbamate insecticides. *J. Agric. Food Chem.* **1999**, *47*, 762−769.

(11) Nishida, S.; Matsuo, N.; Hatakoshi, M.; Kishida, H. (Sumitomo Chemical Co., Ltd.) Nitrogen-containing heterocyclic compounds and their use. Jpn. Kokai Tokkyo Koho 59199673, 1984.

(12) Katagi, T. Experimental and theoretical studies on fenton oxidation of a pyrethroid model ester. *J. Pestic. Sci*. **1992**, *17*, 191−198.
(13) Dewar, M. J. S.; Zoebisch, E. G.; Healy, E. F.; Stewart, J. J. P. AM1: A new general purpose quantum mechanical model. *J. Am. Chem. Soc*. **1985**, *107*, 3902−3909.
(14) Durst, F.; Benveniste, I. Cytochrome P450 in plants. In *Cytochrome P450*; Schenkman, J. B., Greim, H., Eds.; Springer-Verlag: New York, 1993; pp 293−310.
(15) Pudzianowski, A. T.; Loew, G. H. Mechanistic studies of oxene reactions with organic substrates: reaction paths on MNDO enthalpy surface-models for cytchrome P450 oxidations. *Int. J. Quantum Chem.* **1983**, *23*, 1257−1268.
(16) Katagi, T. Application of molecular orbital calculations to the estimation of environmental and metabolic fates of pesticides. In *Structure, Activity, and Ecotoxicology of Agrochemicals*; Draber, W., Fujita, T., Eds.; CRC Press: Boca Raton, FL, 1992; pp 543−564.
(17) Skidmore, M. W.; Ambrus, Á. Pesticide metabolism in crops and livestock. In *Pesticide Residues in Food and Drinking Water: Human Exposure and Risks*; Hamilton, D., Crossley, S., Eds.; Wiley: New York, 2004; pp 63−120.
(18) *Evaluation Report: Pyridalyl*; Pesticides Expert Committee, Food Safety Commission, Cabinet Office Government of Japan: Tokyo, Japan, 2004.
(19) Quistad, G. B.; Staiger, L. E.; Mulholland, K. M.; Schooley, D. A. Plant metabolism of fluvalinate [α-cyano-3-phenoxybenzyl 2-[2-chloro-4-(trifluoromethyl)anilino]-3-methyl-butanoate]. *J. Agric. Food Chem.* **1982**, *30*, 888−895.
(20) Mauchamp, B.; Malosse, C.; Saroglia, P. Biological effects and metabolism of fenoxycarb after treatement of the fourth and the fifth instars of the tabacco budworm, *Heliothis virescens* F. *Pestic. Sci*. **1989**, 283−301.
(21) Mikami, N.; Baba, Y.; Katagi, T.; Miyamoto, J. Metabolism of the synthesis pyrethroid fenpropathrin in plants. *J. Agric. Food Chem*. **1985**, *33*, 980−987.
(22) Furuzawa, K.; Mikami, N.; Yamada, H.; Miyamoto, J. Metabolism of the pyrethroid insecticide cypermethrin in cabbage. *J. Pestic. Sci*. **1986**, *11*, 253−260.
(23) Ohkawa, H.; Kaneko, H.; Miyamoto, J. Metabolism of permethrin in bean plants. *J. Pestic. Sci*. **1977**, *2*, 67−76.
(24) Ohkawa, H.; Nambu, K.; Miyamoto, J. Metabolic fate of fenvalerate (sumicidin) in bean plants. *J. Pestic. Sci.* **1980**, *5*, 215−223.
(25) Gaughan, L. G.; Casida, J. E. Degradation of *trans*- and *cis*-permethrin on cotton and bean plants. *J. Agric. Food Chem.* **1978**, *26*, 525−528.
(26) Lee, P. W.; Stearns, S. M.; Powell, W. R. Metabolic fate of fenvalerate in wheat plants. *J. Agric. Food Chem.* **1988**, *36*, 189−193.
(27) Safari, N.; Bahadoran, F.; Hoseinzadeh, M. R.; Ghiasi, R. Cytchrome P-450 model reaction: effects of substitution on the rate of aromatic hydroxylation. *J. Porphyrins Phthalocyanines* **2000**, *4*, 285−291.
(28) Katagi, T. Theoretical estimation of site specificity in the metabolic hydroxylation of synthetic pyrethroids. *J. Pestic. Sci*. **1990**, *15*, 427−433.
(29) Ackland, M. J. Correlation between site specificity and electrophilic frontier values in the metabolic hydroxylation of biphenyl, di-aromatic and CYP2D6 substrates: a molecular modelling study. *Xenibiotica* **1993**, *23*, 1135−1144.
(30) Keserü, G. M.; Kolossváry, I.; Bertók, B. Cytochrome P-450 catalysed insecticide metabolism. Prediction of regio- and stereoselectivity in the primer metabolism of carbofuran: a theoretical study. *J. Am. Chem. Soc*. **1997**, *119*, 5126−5131.

Received for review February 18, 2005. Revised manuscript received April 21, 2005. Accepted May 1, 2005.

JF0503816